Published in final edited form as:

Hepatology. 2016 November ; 64(5): 1534–1546. doi:10.1002/hep.28659.

Adipocyte-Specific Over-Expression of Retinol-Binding Protein 4 (RBP4) Causes Hepatic Steatosis in Mice

Seung-Ah Lee[1], **Jason J. Yuen**[1], **Hongfeng Jiang**[1], **Barbara B. Kahn**[2], and **William S. Blaner**[1]

[1]Department of Medicine, College of Physicians and Surgeons, Columbia University, 650 W. 168th Street, New York, NY 10032

[2]Division of Endocrinology, Diabetes, and Metabolism, Department of Medicine, Beth Israel Deaconess Medical Center, Harvard Medical School, Boston, MA 02215

Abstract

There is considerable evidence that both retinoids and retinol-binding protein 4 (RBP4) contribute to the development of liver disease. To understand the basis for this, we generated and studied transgenic mice that express human RBP4 (hRBP4) specifically in adipocytes (adi-hRBP4 mice). When fed a chow diet, these mice show an elevation in adipose total RBP4 (mRBP4 + hRBP4) protein levels. However, no significant differences in plasma RBP4 or retinol levels, or differences in hepatic or adipose retinoid (retinol, retinyl ester, and all-*trans*-retinoic acid) levels were observed. Strikingly, male adi-hRBP4 mice fed a standard chow diet display significantly elevated hepatic triglyceride levels at 3-4 months of age compared to matched littermate controls. When mice were fed a high-fat diet, this hepatic phenotype, as well as other metabolic phenotypes (obesity and glucose intolerance) worsened. Since adi-hRBP4 mice have increased TNFα and leptin expression and crown-like structures in adipose tissue, our data are consistent with the notion that adipose tissue is experiencing RBP4-induced inflammation that stimulates increased lipolysis within adipocytes. Our data further establish that elevated hepatic triglyceride levels result from increased hepatic uptake of adipose-derived circulating free fatty acids (FFAs). We obtained no evidence that elevated hepatic triglyceride levels arise from increased hepatic *de novo* lipogenesis, or decreased hepatic FFA oxidation, or decreased very low density lipoprotein (VLDL) secretion.

Conclusion—Our investigations establish that RBP4 expressed in adipocytes induces hepatic steatosis arising from primary effects occurring in adipose tissue.

Keywords

Retinoid; Vitamin A; Glucose Intolerance; Fatty Acid Uptake; and Obesity

---

There is substantial evidence associating elevated circulating levels of retinol-binding protein 4 (RBP4)1 with non-alcoholic fatty liver disease (NAFLD) development (1-6). RBP4 was originally identified and studied as the sole specific transport protein for retinol in the

---

Contact Information: William S. Blaner, Ph.D., Department of Medicine, College of Physicians and Surgeons, Columbia University, 650 W. 168th Street, New York, NY 10032; wsb2@cumc.columbia.edu.

circulation (7). Retinol bound to RBP4 accounts for approximately 95% of the retinoid that is present in the fasting circulation (7). Many investigators have reported findings that associate elevated RBP4 levels with the development of type II diabetes (8-12), cardiovascular disease (13-16), as well as NAFLD (1-6). Kahn and colleagues proposed that the development of obesity leads to increased expression of RBP4 by adipocytes, influencing metabolic disease development (8, 9). A large observational literature, involving diverse patient cohorts, provides evidence for associations between elevated circulating RBP4 levels and NAFLD (1-3). There also is evidence from animal studies establishing that treatment with an agent that reduces circulating RBP4 levels also reduces hepatic steatosis in high-fat diet fed C57BL/6J wild type (4) and *ob*/*ob* genetically obese mice (5). Moreover, infusion of recombinant RBP4 into C57BL/6J mice is reported to induce hepatic SREBP-1c activation and accelerate hepatic lipogenesis and fat accumulation (6). However, it remains to be established whether RBP4 can actually stimulate hepatic steatosis in a liver autonomous manner (17). It also remains to be established whether the relationship between RBP4 and NAFLD may involve the actions of the retinoid, or potentially a non-retinoid, ligand transported by RBP4.

To gain a better understanding of the actions primarily of RBP4 but also of retinoids in inducing NAFLD, we generated a transgenic mouse model that expresses human RBP4 (hRBP4) specifically in adipocytes. When maintained on a conventional chow diet, these mice develop NAFLD by 3 to 4 months of age. When challenged with a high-fat diet, the metabolic phenotype of these transgenic mice worsens more quickly than littermate controls. Our investigations provide new insight into the basis for RBP4-induced NAFLD development.

Experimental Procedures

Targeting Construct and Generation of Adipocyte-specific hRBP4 (adi-hRBP4) Transgenic Mice

To generate adi-hRBP4 transgenic mice, we employed the pROSA26-1 targeting vector obtained from Addgene (Cambridge, MA). A full length cDNA encoding hRBP4 was cloned into pROSA26-1. The hRBP4 cDNA was preceded by a *loxP*-flanked *neo*^{r}-stop cassette, followed by an internal ribosomal entry site-enhanced green fluorescent protein (EGFP) cassette flanked with a *Flp* recombinase-recognition target, and a polyadenylation signal (Figure 1A). More details regarding the generation of adi-RBP4 mice are provided in the Supporting Information.

Quantitative Analysis of Retinol, Retinyl Ester, and Retinoic Acid Concentrations in Liver, Adipose Tissue and Plasma

To assess retinol and individual retinyl ester levels in liver and adipose tissue and retinol levels in plasma, we employed a high performance liquid chromatography (HPLC)-based methodology that has been standardly employed in our laboratory for many years (18).

[1]We will use the designation retinol-binding protein 4 (RBP4) throughout this manuscript. For database searches, the reader should be aware that this protein has also been referred to in the literature as simply retinol-binding protein or RBP.

Tissue retinoic acid concentrations were determined using an ultra high performance liquid chromatography electrospray Ionization-tandem mass spectrometry (LC/MS/MS)-based methodology that we have described (19). This methodology allows for the separation and determination of the all-*trans*-, 13-*cis*- and 9-*cis*-isomers of retinoic acid. In our studies, only detectable levels of all-*trans*-retinoic acid were present in all of the liver and adipose tissue samples analyzed. The low limit of detections for the three retinoic acid isomers were 20 pg/g liver and 30 pg/g adipose tissue. Specific details regarding these HPLC- and LC/MS/MS-based protocols are provided in the Supporting Information.

The Supporting Information also provides detailed descriptions of other experimental protocols employed in our studies including dietary manipulations, metabolic measurements, biochemical analyses, LC/MS/MS analysis of FFAs, histochemical analysis, measurement of adipocyte size, measurement of hepatic *de novo* lipogenesis, assessments of hepatic free fatty acid (FFA) uptake, measurement of ketone bodies, measurement of hepatic very low density lipoprotein (VLDL) production, quantitative PCR, immunoblotting, and statistical analyses.

Results

Generation and Characterization of Adipocyte-specific hRBP4 Transgenic (Adi-hRBP4) Mice

To generate cell type-specific hRBP4 transgenic mice, we adopted a ROSA26 knock-in strategy that allows for expression of a bicistronic message, encoding both a hRBP4 transgene and enhanced green fluorescent protein (EGFP), after removal of a *loxP*-flanked neo^r-stop cassette (Figure 1A). To specifically express hRBP4 in adipocytes, knock-in mice were bred with *adiponectin-Cre* mice (20). Since hRBP4 and EGFP are translated individually from the same mRNA transcript, EGFP expression levels reflect the expression level of hRBP4. To verify transgene expression, tissue extracts were analyzed by Western blotting for EGFP expression (Figure 1B). The EGFP transgene was expressed in visceral (epididymal), subcutaneous (inguinal), and brown adipose tissue (BAT). Transgene expression was not observed in liver or lung (Figure 1B), or in other tissues examined including kidney, heart, skeletal muscle, and spleen. hRBP4 mRNA levels determined by qPCR for visceral fat were comparable to those of endogenous mouse RBP4 mRNA. This resulted in an elevation in total RBP4 (mRBP4 + hRBP4) mRNA expression in visceral adipose tissue in the adi-hRBP4 mice (Figure 1C). Expression of the *hRbp4* transgene did not affect expression of the endogenous *mRbp4* gene. Adipose RBP4 protein levels detected using a pan-anti-RBP4 antibody (Figures 1D and 1E), which possesses equal specificity towards mouse and human RBP4 (Supplementary Figure 1A), showed an increase in adipose tissue total RBP4 (mRBP4 + hRBP4) protein levels. No differences in body weights were observed between male chow-fed 3-4 month old adi-hRBP4 and their littermate controls. NMR analyses established similar body compositions for chow-fed adi-hRBP4 and control mice (Supplementary Figure 1B).

Since RBP4 is the sole specific transport protein for retinol in the circulation, we evaluated parameters associated with the maintenance of retinoid homeostasis in age-matched male adi-hRBP4 and control mice fed a standard chow diet containing 15 IU vitamin A/g chow.

HPLC analysis demonstrated that neither retinol nor retinyl ester levels in liver or visceral adipose tissue were different for chow-fed adi-hRBP4 versus control mice (Table 1). LC/MS/MS analysis showed no strain-dependent differences in all-*trans*-retinoic acid levels for either liver or visceral fat (Table 1 and Figure 1F). Plasma retinol levels also were not different, which is consistent with the notion that plasma RBP4 levels in adi-hRBP4 mice are similar to those of littermate controls. This is further confirmed by Western blot analyses showing comparable plasma RBP4 for the strains fed a chow diet (Figures 7A and 7B). We observed no differences in hepatic mRNA levels for *Aldh1a1*, *Cyp26a1*, *Cyp26b1*, *Rara*, *Rarb*, or *Lrat*, each of which encodes a key protein involved in mediating retinoid metabolism or actions. Thus, with regards to basic parameters associated with the maintenance of retinoid homeostasis, the adi-hRBP4 mice, when fed a chow diet, are not different from littermate controls.

We next investigated whether adipocyte-specific expression of hRBP4 might affect adipose tissue physiology and/or morphology. H&E stained sections of visceral adipose tissue revealed that the adipocytes of chow-fed adi-hRBP4 mice were hypertrophic (Figure 2A). When stained sections were analyzed to determine the cross-sectional area of each adipocyte, adi-hRBP4 mice were found to have a greater number of large adipocytes compared to matched control mice (Figure 2B). This difference was reflected in an approximate 2-fold increase in mean cross-sectional area for adipocytes from adi-hRBP4 mice maintained on a chow diet (Figure 2C). Previous studies have established that hypertrophic adipocytes are more lipolytic, are more resistant to insulin action than small adipocytes, and have an altered pattern of adipokine secretion (21-24). We therefore asked whether expression levels for genes associated with lipolysis were different for adi-hRBP4 mice. We found that mRNA expression of the genes encoding adipocyte triglyceride lipase (*Atgl*) and hormone-sensitive lipase (*Hsl*) were significantly upregulated in visceral fat from adi-hRBP4 mice (Figure 2D). We also observed impaired glucose tolerance in 90-120 day old adi-hRBP4 mice fed a chow diet (Figure 2E). As can be seen in Figure 2F, the areas under the glucose clearance curves (AUCs) were significantly greater for adi-hRBP4 mice following an IP glucose challenge. Thus, expression of the hRBP4 transgene in adipocytes gave rise to altered adipose tissue histology and glucose clearance.

Hepatic Lipid Accumulation is Altered in Adi-hRBP4 Mice

We observed no differences in fasting plasma glucose, TG, TC, or ALT levels for chow-fed adi-hRBP4 mice compared to the control mice. However, fasting plasma FFA levels were significantly elevated in chow-fed adi-hRBP4 mice compared to controls (Figure 3A).

Fasting hepatic TG levels of chow-fed male adi-hRBP4 mice were significantly elevated over those of age- and gender-matched littermates (Figure 3B). Hepatic cholesterol levels also were significantly elevated (Figure 3C), although liver-to-body weight ratios were not different. Cryosections of liver stained with Oil Red O showed an increase in lipid accumulation (Figure 3D). We observed no differences in expression levels for genes associated with hepatic lipid metabolism including *Srebp-1c*, *Pparg*, *Chrebp*, *Fas*, *Acc1*, *Scd1*, *Dgat1*, and *Dgat2*. These differences in hepatic fat accumulation were not observed for chow-fed age-matched female adi-hRBP4 and littermate controls.

We then challenged male mice with a high-fat diet (60% of calories from fat; 4 IU vitamin A/g diet), starting at 7~8 weeks of age. Over a period of 24 days, adi-hRBP4 mice gained significantly more body weight than matched littermates, approximately 10 g versus 7 g (Figure 4A). Statistically significant differences in body weights were identified by 14 days after initiation of high-fat diet feeding, with a significant increase in fat mass identified (Supplementary Figure 1C). Hepatic TG levels were significantly higher in adi-hRBP4 mice than control mice fed the same high-fat diet (Figure 4B). This was confirmed by Oil Red O staining (Figure 4C). High-fat diet-fed adi-hRBP4 mice were also less responsive to a glucose challenge than matched control mice (Supplementary Figures 2A and 2B). Collectively, these data establish that a relatively modest elevation in adipocyte RBP4 expression gives rise to elevated hepatic lipid accumulation and a worsening of glucose tolerance both for chow diet and high-fat diet fed mice.

We next determined by LC/MS/MS plasma and liver FFA levels for adi-hRBP4 mice and littermate controls fed the high-fat diet. Liver FFA levels were significantly elevated in the adi-hRBP4 mice, suggesting increased FFA availability for hepatic TG synthesis (Figure 4D). Plasma FFA levels were also significantly elevated in the adi-hRBP4 mice (Figure 4E). We analyzed the acyl composition of the hepatic FFA pool and determined that the C16:1, C18:1 and C22:6 species were significantly elevated, although most other FFA species trended towards being elevated in high-fat diet fed adi-hRBP4 mice (Figure 4F).

Fatty Acid Uptake Contributes to Hepatic Steatosis in Adi-hRBP4 Mice Fed a High-fat Diet

To understand better the steatosis phenotype of adi-hRBP4 mice, we determined whether livers of adi-hRBP4 mice more readily accumulate a dose of [^{3}H]oleic acid from the circulation. Indeed, livers of adi-hRBP4 mice fed a high-fat diet showed significantly greater accumulation of ^{3}H-cpm in liver lipids (Figure 5A). We also found that mRNA expression of two genes associated with FFA uptake, *Cd36* and *Fabp1*, were elevated in the livers of adi-hRBP4 mice (Figure 5B). These data suggest that increased FFA uptake from the circulation contributes to the observed elevation in hepatic TG levels seen in adi-hRBP4 mice.

The possibility of increased fat synthesis in livers of adi-hRBP mice was evaluated. SREBP-1c protein levels were not elevated (Supplementary Figure 2C). We also obtained no evidence by qPCR analysis of increased mRNA expression levels for other genes involved in hepatic lipogenesis including *Chrebp*, *Pparg*, *Fas*, *Scd1*, *Dgat1* and *Dgat2*. To confirm that there were no changes in hepatic *de novo* lipogenesis in the livers of adi-hRBP4 mice, we undertook direct *in vivo* analysis of hepatic fat synthesis using a well established protocol (25) assessing ^3H_2O incorporation into newly synthesized fat. Agreeing with the qPCR and Western blot data, we did not observe a statistically significant increase in the rate of *de novo* lipogenesis in the livers of adi-hRBP4 mice (Figure 5C).

We further investigated whether lipid utilization by livers of adi-hRBP4 mice may be different from control mice. First, we determined whether hepatic VLDL secretion might be altered in these mice using the total lipase inhibitor P407 to block lipoprotein clearance from the circulation (18, 19). These studies revealed no differences in the rate of VLDL secretion between adi-hRBP4 mice and littermate controls (Supplementary Figure 2D). We also observed no differences in hepatic mRNA expression of *Apob* or *Mttp*, two genes essential

for VLDL secretion. To understand whether there might be a difference in rates of FFA oxidation, we measured hepatic ketone body production in adi-RBP4 and control mice. We did not find statistically significant genotype-dependent differences in FFA oxidation (Supplementary Figure 2E).

Gluconeogenic Gene Expression Is Altered in Liver of adi-hRBP4 mice

We analyzed expression of the key hepatic gluconeogenic enzymes PEPCK and G6Pase (Figures 5D and 5E). Expression of both genes was markedly increased in adi-hRBP4 mice fed a high-fat diet, suggesting an increased rate of hepatic gluconeogenesis for adi-hRBP4 mice. This increase is likely mediated through increased *Foxo1* expression, which was also elevated in adi-hRBP4 liver (Figure 5F).

Adipose hRBP4 Expression in Mice Fed a High-fat Diet Alters Visceral Adipose Tissue Function and Increases Inflammation

Histological analysis of visceral adipose tissue of adi-hRBP4 mice fed a high-fat diet demonstrated more distinct crown-like structures than matched controls fed the same diet (Figure 6A). The crown-like structures are proposed to contribute to adipose inflammation in obesity (26). Compared to chow-fed adi-hRBP4 mice (Figure 2A), the number of crown-like structures present in adipose tissue increased upon high-fat feeding. We also observed a significant elevation of mRNA levels encoding the proinflammatory cytokine TNFα (Figure 6B) as well as TNFα protein levels (Figure 6C) in visceral adipose tissue of adi-hRBP4 mice. However, we did not observe significant differences in plasma TNFα levels between adi-hRBP4 and control mice (Figure 6D). The literature proposes that TNFα activates lipolysis in visceral adipose tissue, resulting in elevated circulating FFA levels and contributing to an enlarged hepatic FFA pool that is used for TG synthesis (27, 28). Moreover, plasma levels of leptin were significantly elevated over those of littermate controls when adi-hRBP4 mice were fed a high-fat diet (Figure 6E), consistent with their increased adiposity (see Supplementary Figure 1C).

Retinoid Homeostasis is Significantly Altered upon High-fat Feeding

The effects of feeding a high-fat diet for 10 weeks on retinoid homeostasis in adi-hRBP4 and control mice were investigated. Hepatic retinyl ester levels were diminished for both genotypes by approximately 60% compared to feeding a chow diet. However, no differences between genotypes were observed (Table 1). We note that the chow diet provides approximately 3-times more vitamin A than the high-fat diet, so this lowering of hepatic retinyl ester levels might be expected. Hepatic retinol levels were significantly diminished in the high-fat fed mice, as were adipose tissue retinyl ester levels (Table 1). This was accompanied by a significant increase (approximate doubling) in plasma retinol levels for both high-fat fed adi-hRBP4 mice and littermate controls. The increase in plasma retinol correlates well with an observed increase in circulating levels of RBP4 (Figures 7A and 7B). High-fat feeding did not increase mRNA expression levels of the human hRBP4 transgene. However, our analyses showed that mRNA expression of *Aldh1a1, Cyp26a1, Cyp26B1*, and *Rarb* were significantly increased in the livers of adi-hRBP4 mice (Figure 7C), possibly suggesting increased hepatic all-*trans*-retinoic acid synthesis. However, steady-state hepatic

all-*trans*-retinoic acid levels were lower in livers from adi-hRBP4 mice fed the high-fat diet compared to controls (Table 1).

Discussion

With the reports from Yang et al. (8) and Graham et al. (9) a decade ago, there has been considerable research interest focused on understanding how RBP4 synthesized by adipocytes contributes to the development of metabolic disease, including liver disease. Although much of this literature reports associations between elevated serum/plasma and/or tissue RBP4 levels and metabolic disease (1-6, 8-16), there are a number of studies reporting evidence to the contrary (29-32), including ones that failed to establish associations between RBP4 and NAFLD (33, 34). Undoubtedly some of this disagreement in the literature arises from differences in methodologies employed by different research groups, including methodologies needed for grouping and studying human subjects as well as laboratory techniques used to evaluate RBP4 levels and actions (35-37). To better understand the role of RBP4 in metabolic disease, we generated and studied adi-hRBP4 mice that express hRBP4 specifically in adipocytes. Although the adi-hRBP4 mice when fed a chow diet show a modest elevation (see Figure 1D and 1E) in adipose tissue total RBP4 (mRBP4 + hRBP) protein levels and no statistically significant change in plasma total RBP4 or retinol levels, these mice accumulate significantly more hepatic fat and are significantly less glucose tolerant than matched littermate controls fed a chow diet. Thus, our data directly establish that elevated expression of RBP4 in adipocytes gives rise to adverse metabolic consequences prior to a detectable elevation in circulating RBP4 levels.

Earlier published studies exploring linkages between RBP4 and hepatic steatosis have primarily focused on elevated circulating RBP4 levels. The present work is important because it demonstrates that disease development (insulin resistance and hepatic steatosis) occurs before an elevation in circulating RBP4 can be detected and that elevation of RBP4 selectively in adipocytes has profound effects in the liver and systemically. We propose that the disease process does not commence after circulating RBP4 levels rise to some elevated level. Rather, hepatic disease can commence earlier, as RBP4 levels within adipose tissue become elevated, before elevations in circulating RBP4 levels can be detected. Our data do not disprove the notion that high circulating RBP4 levels *per se* may have an important casual role in the development of hepatic steatosis. As seen in Figure 7, Panel B, circulating RBP4 levels are significantly elevated in adi-hRBP4 mice fed a high-fat diet. We note that the magnitude of these changes are similar to those originally reported more than a decade ago by Kahn and colleagues (8, 9). Based on our present studies and the literature, we believe that the role of RBP4 in inducing metabolic disease is both complex and multifaceted. The present studies underscore this complexity.

Differences in retinoid homeostasis in liver and adipose tissue do not account for the elevations in hepatic fat accumulation observed for adi-hRBP4 mice fed a chow diet. Table 1 establishes that steady state hepatic and adipose levels of retinol, retinyl esters and all-*trans*-retinoic acid levels are not different for the two groups. Plasma retinol and RBP4 levels also were not different for the two groups. Moreover, we observed no differences in hepatic gene expression levels for the canonical retinoic acid-responsive genes *Aldh1a1*, *Cyp26a1,*

Cyp26B1, RARa, Rarb, and *Lrat* (38). These data indicate that alterations in hepatic retinoid signaling do not account for the fatty liver phenotype of chow-fed adi-hRBP4 mice. Rather, it appears that RBP4 itself is acting locally within adipose tissue to bring about the elevated fat levels observed in livers of adi-hRBP4 mice. Moraes-Vieira et al., based on studies of hRBP4 transgenic mice that possess high circulating levels of hRBP4 (transgenically overexpressed and secreted from skeletal muscle), concluded that RBP4 can activate antigen-presenting cells within adipose tissue leading to adipose inflammation (39). As assessed by the increase in both *Tnfa* mRNA and protein levels, the adipose depots of chow-fed adi-hRBP4 mice are experiencing inflammation.

For both chow fed and high-fat diet fed adi-hRBP4 mice, we observed increased adipose tissue expression of *Atgl* and *Hsl*, the two lipases that are primarily responsible for the hydrolysis of adipose triglyceride (40, 41). This, we propose, leads to increased mobilization of FFAs from adipocytes of adi-hRBP4 mice, as evidenced by an elevation in fasting plasma FFA levels. This elevation in circulating FFAs contributes to increased FFA uptake and accumulation by the liver, where expression of the plasma membrane FFA transporter *Cd36* and the intracellular FFA transporter *Fabp1* are both elevated. Thus, even when mice are fed a standard chow diet, an increase in RBP4 expression in adipocytes gives rise to a cascade of responses that bring about a redistribution of FFA from adipose tissue to liver, resulting in excessive hepatic fat accumulation.

Ahmadian et al., reported that adipocyte-specific overexpression of ATGL improved insulin sensitivity and gave rise to lower hepatic triglyceride levels (42). However, the relationship between adipocyte expression of ATGL and hepatic triglyceride accumulation is a complicated one. Schoiswohl et al. recently reported that mice in which ATGL expression was ablated specifically in adipocytes show less hepatic triglyceride accumulation than control mice, upon both chow diet and high-fat diet administration (43). Thus, both overexpression and complete ablation of ATGL in adipocytes are reported to lessen hepatic triglyceride accumulation. Interestingly and in agreement with our data for adi-hRBP4 mice, both Ahmadian et al. (42) and Schoiswohl et al. (43) failed to observe an effect of high-fat diet feeding on circulating plasma FFA levels for either their control or transgenic mice. Kim et al. reported that an improvement in metabolic parameters was observed in ob/ob mice overexpressing adiponectin specifically in adipocytes (44). This was associated with an increase in HSL expression. The findings from Ahmadian et al. (42) and Kim et al. (44) are in apparent contradiction to our findings where we propose that an elevation in adipocyte ATGL and HSL expression contributes to increased hepatic triglyceride accumulation. Importantly, the transgenic models studied by Ahmadian et al. (42) and Kim et al. (44) have a very different adipose phenotype compared to the adi-hRBP4 mice. The adipocytes present in adi-hRBP4 mice are much larger than those of matched controls. Whereas, both Ahmadian et al. and Kim et al. report that the adipocytes present in their transgenic mouse models are much smaller than those of matched controls. The literature is clear that hypertrophic adipocytes are more lipolytic, are more resistant to insulin action than small adipocytes, and have an altered pattern of adipokine secretion (21-24). This difference, and possibly other differences in adipocyte physiology, undoubtedly account for the apparent discrepancies between our findings for adi-hRBP4 mice and those reported by Ahmadian et al. (42) and Kim et al. (43). Our data also are consistent with human genetic studies showing

that single nucleotide polymorphisms in the *RBP4* gene which increase RBP4 expression in adipose tissue are associated with increased susceptibility to insulin resistance and type 2 diabetes (11).

When adi-hRBP4 mice were metabolically stressed with a high-fat diet, many of their metabolic parameters worsened, including ones associated with hepatic fat accumulation. Although no significant differences in body weights between adi-hRBP4 and littermate controls were observed when mice were maintained on a chow diet, when fed a high-fat diet, the adi-hRBP4 mice gained more weight than controls within 14 days of the start of high-fat diet feeding. The high-fat diet fed adi-hRBP4 mice also were less tolerant of a glucose challenge than matched control mice. Histological analyses of adipose tissue from high-fat fed adi-hRBP4 mice show an increased presence of “crown-like' structures which are indicative of increased adipose tissue inflammation (27, 28). *Tnf*α mRNA and TNFα protein levels were elevated in adipose tissue of high-fat fed adi-hRBP4 mice. This was accompanied further by significantly higher circulating plasma leptin concentrations. It is well established that elevated adipocyte expression of TNFα gives rise to increased leptin secretion from these cells and elevated circulating leptin levels (28). Based on the findings of Moraes-Vieira et al. (39) and our present data, it seems reasonable to propose that the high-fat diet fed adi-RBP4 mice experienced RBP4-induced systemic inflammation that worsens the metabolic phenotype of the mice.

We systematically explored the molecular basis for the elevation in hepatic triglyceride levels in adi-hRBP4 mice fed a high-fat diet. We obtained no evidence for an increase in hepatic *de novo* lipogenesis, nor did we detect differences in genes/proteins important to *de novo* lipogenesis. We also obtained no evidence that a decreased rate of utilization of hepatic triglyceride contributes to the increased hepatic triglyceride accumulation observed in adi-hRBP4 mice. Our data indicate that adi-hRBP4 and control mice utilize FFAs as energy sources at similar rates. No differences in the rate of triglyceride export from the liver via nascent VLDL were observed. However, when we assessed hepatic uptake of ^{3}H-labeled oleic acid from circulations of adi-hRBP4 and control mice, the livers of adi-hRBP4 mice took up more of the labeled FFAs. This experiment, coupled with our qPCR data, support the conclusion that increased hepatic uptake of circulating FFAs accounts substantially for the fatty liver phenotype observed in the adi-hRBP4 mice.

Maher (17) raised a question as to whether RBP4 can actually stimulate hepatic steatosis and in a liver autonomous manner. Our data establish that RBP4 does indeed stimulate hepatic steatosis. However, this effect appears initially to involve RBP4 actions in adipose tissue and not its direct actions in the liver. Also, RBP4 actions in stimulating hepatic steatosis are at least initially independent of its role as a retinoid transport protein in the circulation. This is consistent with data showing that apo-RBP4 is as potent as holo-RBP4 in activating the innate and adaptive immune responses (39, 45). When nutritionally stressed with a high-fat diet, the effects of increased RBP4 expression specifically by adipocytes become more broad. These include increases in circulating retinol and RBP4 levels, as well as levels of the proinflammatory adipokine leptin. Progressively, these changes contribute to a worsening of hepatic steatosis and other aspects of the metabolic phenotype (obesity and glucose intolerance) observed in metabolically stressed adi-hRBP4 mice.

Supplementary Material

Refer to Web version on PubMed Central for supplementary material.

Acknowledgments

Financial Support: This work was supported by U.S. Public Health Services, National Institutes of Health grants R01 DK068437 and R21 AA021336 (to WSB) and R01 DK043051 (to BBK).

References

1. Stefan N, Hennige AM, Staiger H, Machann J, Schick F, Schleicher E, et al. High circulating retinol-binding protein 4 is associated with elevated liver fat but not with total, subcutaneous, visceral, or intramyocellular fat in humans. Diabetes Care. 2007; 30:1173–1178. [PubMed: 17259477]
2. Seo JA, Kim NH, Park SY, Kim HY, Ryu OH, Lee KW, et al. Serum retinol-binding protein 4 levels are elevated in non-alcoholic fatty liver disease. Clin Endocrinol. 2007; 68:555–560.
3. Terra X, Auguet T, Broch M, Sabech F, Hernandez M, Pastor RM, et al. Retinol binding protein 4 circulating levels were higher in nonalcoholic fatty liver disease versus histologically normal liver from morbidly obese women. Obesity. 2013; 21:170–177. [PubMed: 23505183]
4. Preitner F, Mody N, Graham TE, Peroni OD, Kahn BB. Long-term fenretinide treatment prevents high-fat diet-induced obesity, insulin resistance, and hepatic steatosis. Am J Physiol Endocrinol Metab. 2009; 297:E1420–E1429. [PubMed: 19826103]
5. Koh IU, Jun HS, Choi JS, Lim JH, Kim WH, Yoon JB, et al. Fenretinide ameliorates insulin resistance and fatty liver in obese mice. Biol Pharm Bull. 2012; 35:369–375. [PubMed: 22382323]
6. Xia M, Liu Y, Guo H, Wang D, Wang Y, Ling W. Retinol binding protein 4 stimulates hepatic sterol regulatory element-binding protein 1 and increases lipogenesis through the peroxisome proliferator-activated receptor-γ coactivator 1β-dependent pathway. Hepatology. 2013; 58:564–575. [PubMed: 23300015]
7. Blaner WS. Retinol-binding protein: The serum transport protein for vitamin A. Endocr Rev. 1989; 10:308–316. [PubMed: 2550213]
8. Yang Q, Graham TE, Mody N, Preitner F, Peroni OD, Zabolotny JM, et al. Serum retinol binding protein 4 contributes to insulin resistance in obesity and type 2 diabetes. Nature. 2005; 436:356–362. [PubMed: 16034410]
9. Graham TE, Yang Q, BlÜher M, Hammarstedt A, Ciaraldi TP, Henry RR, et al. Retinol-binding protein 4 and insulin resistance in lean, obese, and diabetic subject. N Engl J Med. 2006; 354:2552–2563. [PubMed: 16775236]
10. Cho YM, Youn BS, Lee H, Lee N, Min SS, Kwak SH, et al. Plasma retinol-binding protein-4 concentrations are elevated in human subjects with impaired glucose tolerance and type 2 diabetes. Diabetes Care. 2006; 29:2457–2461. [PubMed: 17065684]
11. Kovacs P, Geyer M, Berndt J, Klöting N, Graham TE, Böttcher Y, et al. Effects of genetic variation in the human retinol binding protein-4 gene (RBP4) on insulin resistance and fat depot-specific mRNA expression. Diabetes. 2007; 56:3095–3100. [PubMed: 17728376]
12. Mody N, Graham TE, Tsuji Y, Yang Q, Kahn BB. Decreased clearance of serum retinol-binding protein and elevated levels of transthyretin in insulin-resistant *ob/ob* mice. Am J Physiol Endocrinol Metab. 2008; 294:E785–E793. [PubMed: 18285525]
13. Bobbert P, Weithäuser A, Anders J, Bobbert T, KÜhl U, Schultheiss HP, et al. Increased plasma retinol binding protein 4 levels in patients with inflammatory cardiomyopathy. Eur J Heart Failure. 2009; 11:1163–1168.
14. Sun Q, Kiernan UA, Shi L, Phillips DA, Kahn BB, Hu FB, et al. Plasma retinol-binding protein 4 (RBP4) levels and risk of coronary heart disease. A prospective analysis among women in the Nurses' Health Study Circulation. 2013; 127:1938–1947. [PubMed: 23584360]
15. Farjo KM, Farjo RA, Halsey S, Moiseyev G, Ma JX. Retinol-binding protein 4 induces inflammation in human endothelial cells by an NADPH oxidase- and nuclear factor kappa B-

dependent and retinol-independent mechanism. Mol Cell Biol. 2012; 32:5103–5115. [PubMed: 23071093]

16. Du M, Otalora L, Martin AA, Moiseyev G, Vanlandingham P, Wang Q, et al. Transgenic mice overexpressing serum retinol-binding protein develop progressive retinal degeneration through a retinoid-independent mechanism. Mol Cell Biol. 2015; 35:2771–2789. [PubMed: 26055327]
17. Maher JJ. Retinol binding protein 4 and fatty liver: A direct link? Hepatology. 2013; 58:477–479. [PubMed: 23703940]
18. O'Byrne SM, Wongsiriroj N, Libien J, Vogel S, Goldberg IJ, Baehr W, et al. Retinoid absorption and storage is impaired in mice lacking lecithin:retinol acyltransferase (LRAT). J Biol Chem. 2005; 280:35647–35657. [PubMed: 16115871]
19. Wongsiriroj N, Jiang H, Piantedosi R, Yang KJ, Kluwe J, Schwabe RF, et al. Genetic dissection of retinoid esterification and accumulation in the liver and adipose tissue. J Lipid Res. 2014; 55:104–114. [PubMed: 24186946]
20. Sasaki Y, de Rudder E, Hobeika E, Pelanda R, Reth M, Rajewsky K, et al. Canonical NF-κB activity, dispensable for B cell development, replaces BAFF-receptor signals and promotes B cell proliferation upon activation. Immunity. 2006; 24:729–739. [PubMed: 16782029]
21. Farnier C, Krief S, Blache M, Diot-Dupuy F, Mory G, Ferre P, et al. Adipocyte functions are modulated by cell size change: potential involvement of an integrin/ERK signaling pathway. Int J Obes Relat Metab Disord. 2003; 27:1178–1186. [PubMed: 14513065]
22. Franck N, Stenkula KG, Ost A, Lindström T, Strålfors P, Nystrom FH. Insulin-induced GLUT4 translocation to the plasma membrane is blunted in large compared with small primary fat cells isolated from the same individual. Diabetologia. 2007; 50:1716–1722. [PubMed: 17572871]
23. Jernås M, Palming J, Sjöholm K, Jennische E, Svensson PA, Gabrielsson BG, et al. Separation of human adipocytes by size: hypertrophic fat cells display distinct gene expression. FASEB J. 2006; 20:1540–1542. [PubMed: 16754744]
24. Skurk T, Alberti-Huber C, Herder C, Hauner H. Relationship between adipocyte size and adipokine expression and secretion. J Clin Endocrinol Metab. 2007; 92:1023–1033. [PubMed: 17164304]
25. Spady DK, Dietschy JM. Sterol synthesis in vivo in 18 tissues of the squirrel monkey, guinea pig, rabbit, hamster, and rat. J Lipid Res. 1983; 24:303–315. [PubMed: 6842086]
26. Kolak M, Wsterbacka J, Velagapudi VR, Wågsäter D, Yetukuri L, Makkonen J, et al. Adipose tissue inflammation and increased ceramide content characterize subjects with high liver fat content independent of obesity. Diabetes. 2007; 56:1960–1968. [PubMed: 17620421]
27. Shang HH, Halbleib M, Ahmad F, Manganiello VC, Greenberg AS. Tumor necrosis factor-α stimulates lipolysis in differentiated human adipocytes through activation of extracellular signal-related kinase and elevation of intracellular cAMP. Diabetes. 2002; 51:2929–2935. [PubMed: 12351429]
28. Kirchgessner TG, Uysal KT, Wiesbrock SM, Marino MW, Hotamisligil GS. Tumor necrosis factor-α contributes to obesity-related hyperleptinemia by regulating leptin release from adipocytes. J Clin Invest. 1997; 100:2777–2782. [PubMed: 9389742]
29. von Eynatten M, Lepper PM, Liu D, Lang K, Baumann M, Nawroth PP, et al. Retinol-binding protein 4 is associated with components of the metabolic syndrome, but not with insulin resistance, in men with type 2 diabetes or coronary artery disease. Diabetologia. 2007; 50:1930–1937. [PubMed: 17639305]
30. Yao-Borengasser A, Varma V, Bodles AM, Rasouli N, Phanavanh B, Lee MJ, et al. Retinol binding protein 4 expression in humans: Relationship to insulin resistance, inflammation, and response to pioglitazone. J Clin Endocrinol Metab. 2007; 92:2590–2597. [PubMed: 17595259]
31. Gómez-Ambrosi J, Rodriquez A, Catalán V, Ramirez B, Silva C, Rotellar F, et al. Serum retinol-binding protein 4 is not increased in obesity or obesity-associated type 2 diabetes mellitus, but is reduced after relevant reduction in body fat following gastric bypass. Clin Endocrinol. 2008; 69:208–215.
32. Motani A, Wang Z, Conn M, Siegler JK, Zhang Y, Liu Q, et al. Identification and characterization of a non-retinoid ligand for retinol-binding protein 4 which lowers serum retinol-binding protein 4 levels *in vivo*. J Biol Chem. 2009; 284:76737670.

33. Kashyap SR, Diab DL, Baker AR, Yerian L, Bajaj H, Gray-McGuire C, et al. Triglyceride levels and not adipokine concentrations are closely related to severity of nonalcoholic fatty liver disease in an obesity surgery cohort. Obesity (Silver Spring). 2009; 17:1696–1701. [PubMed: 19360015]
34. Cengiz C, Ardicoglu Y, Bulut S, Boyacioglu S. Serum retinol-binding protein 4 in patients with nonalcoholic fatty liver disease: does it have a significant impact on pathogenesis? Eur J Gastroenterol Hepatol. 2010; 22:813–819. [PubMed: 19820404]
35. Graham TE, Wason CJ, Blüher M, Kahn BB. Shortcomings in methodology complicate measurements of serum retinol binding protein (RBP4) in insulin-resistant human subject. Diabetologia. 2007; 50:814–823. [PubMed: 17294166]
36. Kotnik P, Fischer-Posovszky P, Wabitsch M. RBP4: a controversial adipokine. Eur J Endocrinol. 2011; 165:703–711. [PubMed: 21835764]
37. Yang Q, Eskurza I, Kiernan UA, Phillips DA, Blüher M, Graham TE, et al. Quantitative measurement of full-length and C-terminal proteolyzed RBP4 in serum of normal and insulin-resistant humans using a novel mass spectrometry immunoassay. Endocrinology. 2012; 153:1519–1527. [PubMed: 22253430]
38. Balmer JE, Blomhoff R. Gene expression regulation by retinoic acid. J Lipid Res. 2002; 43:1773–808. [PubMed: 12401878]
39. Moraes-Vieira PM, Yore MM, Dwyer PM, Syed I, Aryal P, Kahn BB. RBP4 activates antigen-presenting cells, leading to adipose tissue inflammation and systemic insulin resistance. Cell Metabolism. 2014; 19:512–526. [PubMed: 24606904]
40. Lampidonis AD, Rogdakis E, Voutsinas GE, Stravopodis DJ. The resurgence of Hormone-Sensitive Lipase (HSL) in mammalian lipolysis. Gene. 2011; 477:1–11. [PubMed: 21241784]
41. Lass A, Zimmermann R, Oberer M, Zechner R. Lipolysis – A highly regulated multi-enzyme complex mediates the catabolism of cellular fat stores. Progress in Lipid Research. 2011; 50:14–27. [PubMed: 21087632]
42. Ahmadian M, Duncan RE, Varady KA, Frasson D, Hellerstein MK, Birkenfeld AL, et al. Adipose overexpression of desnutrin promotes fatty acid use and attenuates diet-induced obesity. Diabetes. 2009; 58:855–866. [PubMed: 19136649]
43. Schoiswohl G, Stefanovic-Racic M, Menke MN, Wills RC, Surlow BA, Basantani MK, et al. Impact of reduced ATGL-mediated adipocyte lipolysis on obesity-associated insulin resistance and inflammation in male mice. Endocrinology. 2015; 156:3610–3624. [PubMed: 26196542]
44. Kim JY, van de Wall E, Laplante M, Azzara A, Trujillo ME, Hofmann SM, et al. Obesity-associated improvements in metabolic profile through expansion of adipose tissue. J Clin Invest. 2007; 117:2621–2637. [PubMed: 17717599]
45. Norseen J, Hosooka T, Hammarstedt A, Yore MM, Kant S, Aryal P, et al. Retinol-binding protein 4 inhibits insulin signaling in adipocytes by inducing proinflammatory cytokines in macrophages through a c-Jun N-terminal kinase- and toll-like receptor 4-dependent and retinol-independent mechanism. Mol Cell Biol. 2012; 32:2010–2019. [PubMed: 22431523]

List of Abbreviations

RBP4	retinol-binding protein 4
adi-hRBP4	adipocyte-specific human RBP4
mRBP4	mouse RBP4
FFA	free fatty acid
RARs	retinoic acid receptors
RARα	retinoic acid receptor alpha
Aldh1a1	aldehyde dehydrogenase 1A1

Srebp-1c	sterol regulatory element-binding protein-1c
NAFLD	non-alcoholic fatty liver disease
EGFP	enhanced green fluorescent protein
IP	intraperitoneal
TG	triglycerides
TC	total cholesterol
ALT	alanine transaminase
TNFα	tumor necrosis factor-α
HPLC	high-performance liquid chromatography
LC/MS/MS	liquid chromatography tandem mass spectrometry
ATRA-d5	penta-deuterated all-*trans*-retinoic acid
H&E	hematoxylin and eosin
TLC	thin layer chromatography
BSA	bovine serum albumin
PBS	phosphate buffered saline
TCA	trichloroacetic acid
VLDL	very low density lipoprotein
VISC	visceral (epididymal)
SubQ	subcutaneous (inguinal)
BAT	brown adipose tissue
Atgl	adipocyte triglyceride lipase
Hsl	hormone-sensitive lipase
Lpl	lipoprotein lipase
Pparg	peroxisome proliferator-activated receptor gamma
Fas	fatty acid synthase
Acc1	acetyl-CoA carboxylase 1
Scd1	stearoyl-CoA desaturase 1
Dgat1	diglyceride acyltransferase 1
Dagt2	diglyceride acyltransferase 2

Cd36	cluster of differentiation 36
Fabp1	fatty acid-binding protein 1
Apob	apolipoprotein B
Mttp	microsomal triglyceride transfer protein
Pepck	phosphoenolpyruvate carboxykinase
G6Pase	glucose 6-phosphatase
FoxO1	forkhead box O1
Cyp26a1	cytochrome P450, family 26, subfamily a, polypeptide 1
Cyp26b1	cytochrome P450, family 26, subfamily b, polypeptide 1
Rarb	retinoic acid receptor beta
Rbpr2	RBP4 receptor-2
VISC	visceral adipose tissue
ROH	all-*trans*-retinol
RE	retinyl esters
ATRA	all-*trans*-retinoic acid

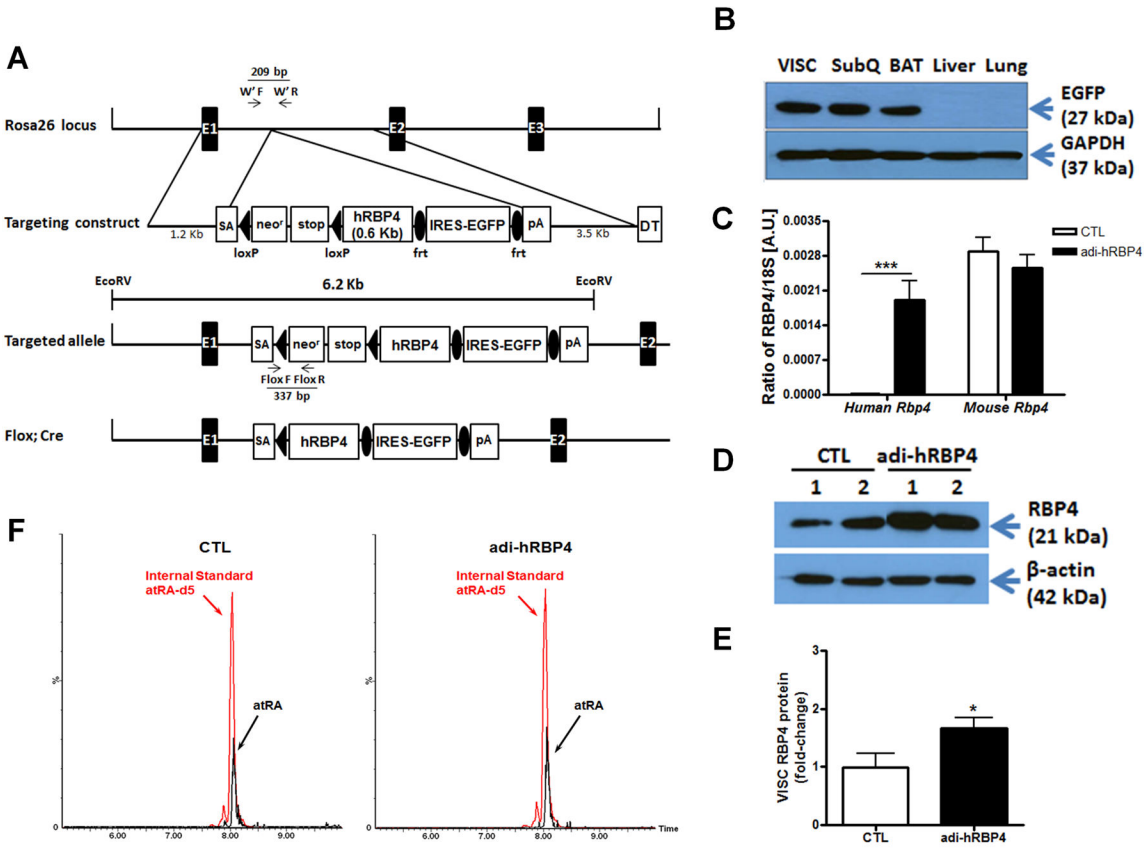

Figure 1. Targeting strategy of the endogenous ROSA26 hRBP4 knock-in mice and properties of the adipose tissue-specific hRBP4 (adi-hRBP4) transgenic mice

(A) Schematic representation for the recombinant hRBP4 alleles. The arrows indicate the positions of the PCR primers used for genotyping. EX 1-3, ROSA26 exons; SA, splice acceptor; DT, diphtheria toxin. (B) Immunoblots showing EGFP protein expression in visceral (VISC), subcutaneous (SubQ) and brown adipose tissue (BAT) but not in liver or lung of adi-hRBP4 mice. (C) Relative mRNA expression of human and mouse RBP4 in visceral fat (VISC) was determined by qPCR in adi-hRBP4 and littermate control (CTL) mice. ***, $P < 0.005$ versus control. (D) Immunoblots showing total RBP4 (mRBP4 + hRBP4) protein expression in visceral fat (VISC) from 2 adi-hRBP4 and 2 littermate control (CTL) mice. (E) Mean visceral fat (VISC) total RBP4 (mRBP4 + hRBP4) protein expression as a ratio to β actin for scanned immunoblots. *, $P < 0.05$ versus control. (F) LC/MS/MS profiles for all-*trans*-retinoic acid (atRA) present in visceral fat from chow-fed adi-hRBP4 and littermate control (CTL) mice. All-*trans*-retinoic acid was detected and quantified using the multiple reaction monitoring mode (MRM) employing the following transitions: all-*trans*-retinoic acid, *m/z* 301.16→123.00; and the internal standard penta-deuterated all-*trans*-retinoic acid (atRA-d5), *m/z* 306.15→127.03.

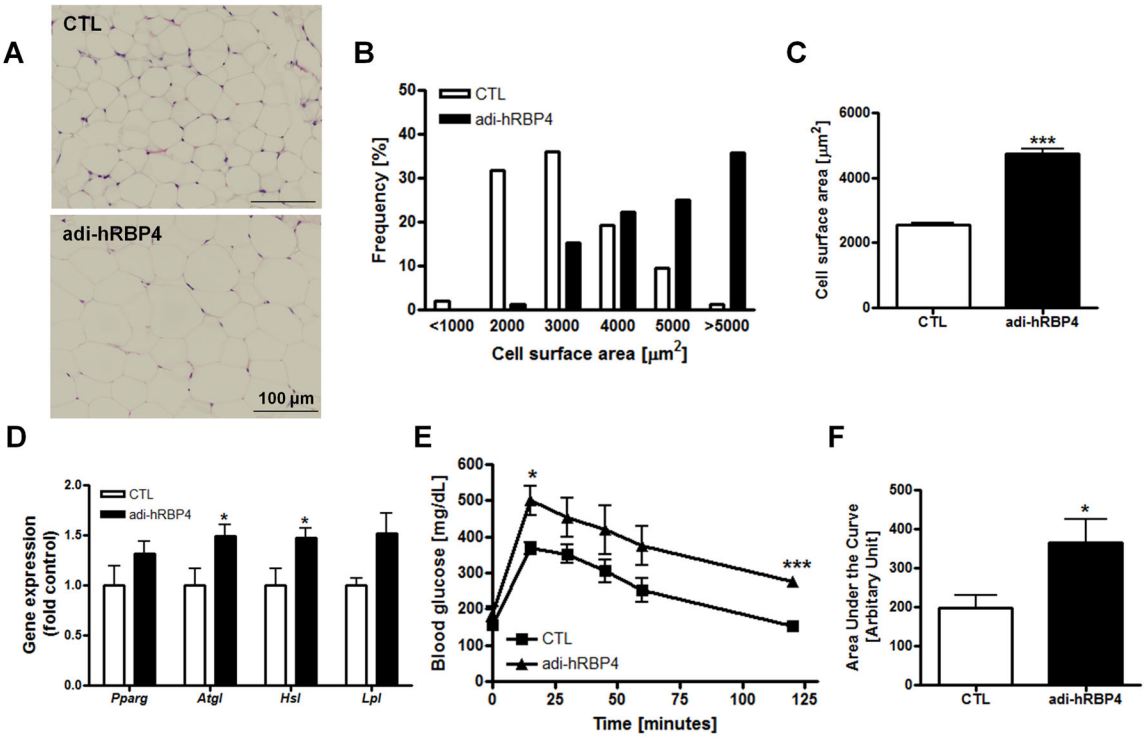

Figure 2. Adipocyte physiology and glucose metabolism are altered in adi-hRBP4 mice fed a chow diet

(A) Representative hematoxylin and eosin (H&E)-stained sections for visceral adipose tissue. Bars represent 100 µm. Frequency distribution of adipocyte cross-sectional areas (B) and mean cross-sectional areas of adipocytes (C). Greater than 100 cells were measured for each of 2 adi-hRBP4 and 2 littermate control mice. (D) mRNA expression of genes encoding lipolysis-related proteins in visceral fat as determined by qT-PCR; n = 6 - 7. All data are normalized to 18S rRNA. *, $P < 0.05$ versus controls (CTL). (E) Glucose tolerance tests (GTT) and (F) the area under the curves (AUCs) (intraperitoneal injection of 2g/kg body weight; 6 h after food removal) (n = 5 - 13). *, $P < 0.05$ versus controls (CTL). Data are presented as means ± SEM.

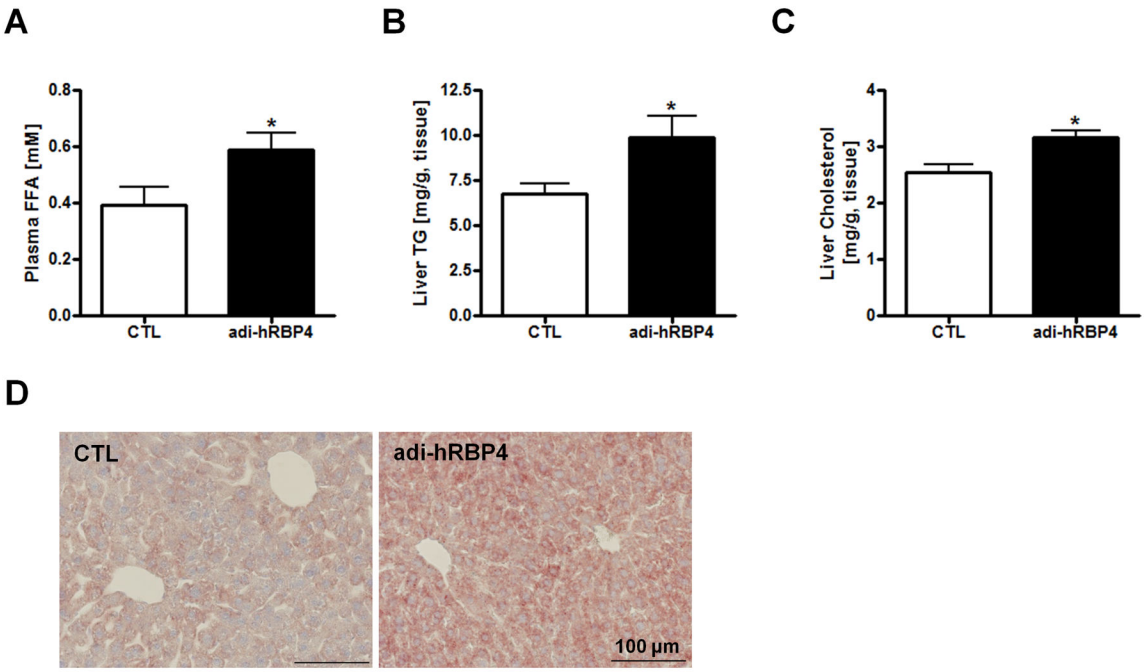

Figure 3. Hepatic lipid deposition is altered in adi-hRBP4 mice

Plasma FFA (A), liver TG (B) and liver total cholesterol (C) levels 6 h after food removal in adi-hRBP4 and littermate control (CTL) mice fed a chow diet throughout life (n = 5 - 13). (D) Representative cryosections of livers stained with Oil Red O. Bars represent 100 μm. *, $P < 0.05$ versus controls.

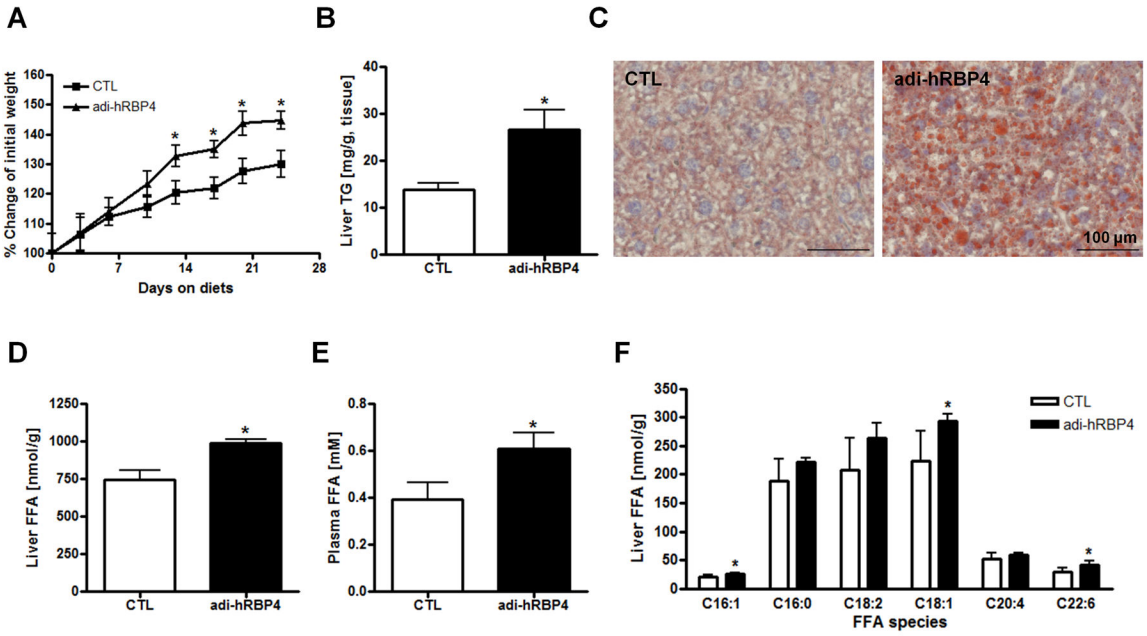

Figure 4. Worsening of the metabolic phenotypes in adi-hRBP4 mice fed a high-fat diet

(A) Weight gains for male adi-hRBP4 and littermate control mice fed a high-fat diet providing 60% of calories from fat. The values presented reflect mean percent weight gains ± SEM. (B) Liver TG levels after a 6 h fast for matched control and adi-hRBP4 mice fed a high-fat diet for 24 days (n = 4 - 6). (C) Representative cryosections of livers stained with Oil Red O in high-fat diet fed mice. Bars represent 100 μM. Total liver FFA (D) levels and plasma FFA (E) levels measured for age- and gender-matched adi-RBP4 and littermate control mice fed a high-fat diet (n = 4 - 6). (F) Acyl composition of the FFA pool within livers of matched adi-RBP4 and littermate control mice as determined by LC/MS/MS (n = 4 - 6). *, $P < 0.05$ versus controls (CTL).

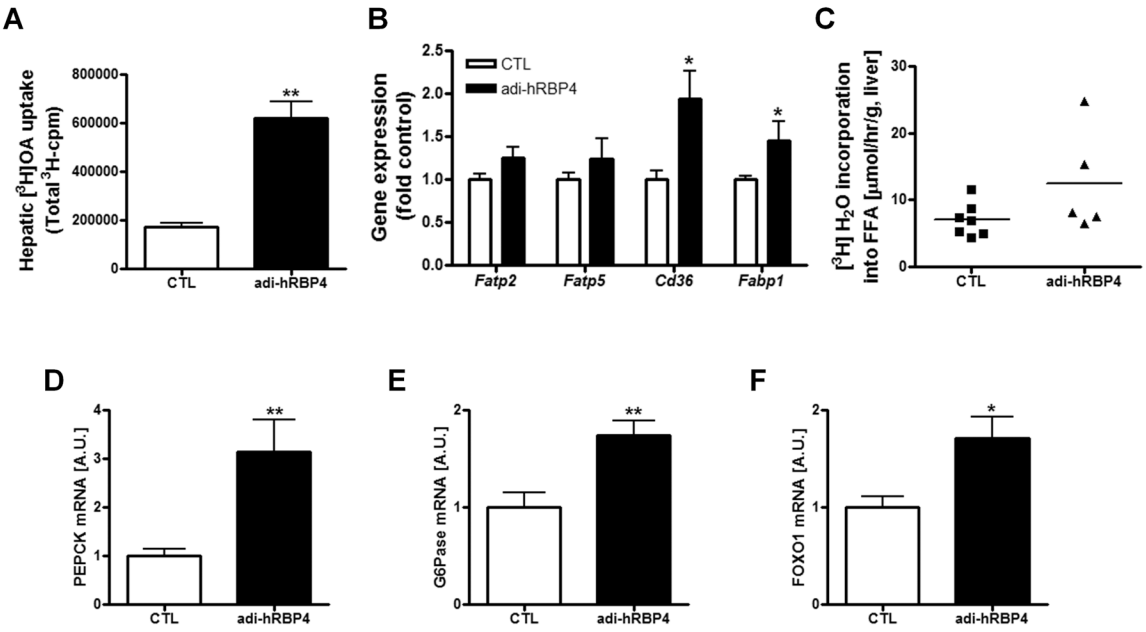

Figure 5. Fatty acid uptake contributes to hepatic steatosis in adi-hRBP4 mice fed a high-fat diet and hepatic gluconeogenic genes are markedly increased

(A) FFA uptake into the livers of matched adi-RBP4 and littermate control mice was quantified by assessing ^{3}H-cpm (n = 3 - 6) 5 minutes after an iv injection of [^{3}H]oleic acid. (B) mRNA expression of genes related to FFA uptake in liver as determined by qPCR (n = 4 - 6). (C) The rate of hepatic *de novo* lipogenesis for matched high-fat fed adi-RBP4 and littermate control mice as quantified by measuring [^{3}H]H_2O incorporated into lipid (n = 6 - 7). mRNA levels of the key hepatic gluconeogenic genes *Pepck* (D) and G6Pase (E) as well as *Foxo1* (F) were determined for liver by qPCR (n = 4 - 6) for matched high-fat diet fed adi-hRBP4 and littermate controls. *, $P < 0.05$; **, $P < 0.01$ versus controls (CTL). AU, Arbitrary units. Data are expressed as means ± SEM.

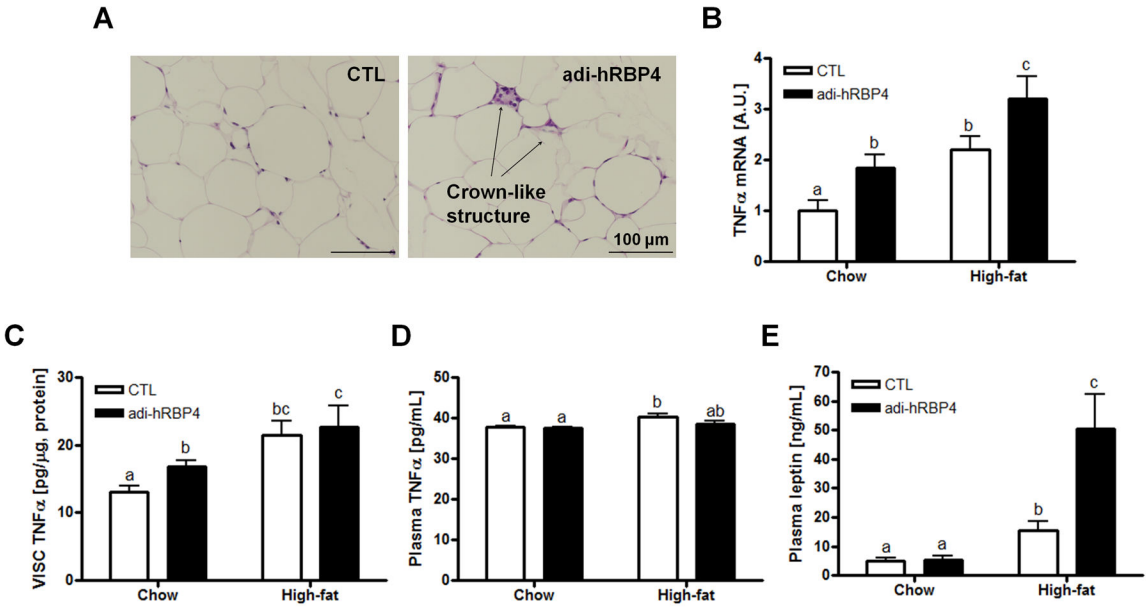

Figure 6. hRBP4 expression in adipose tissue of mice fed a high-fat diet alters visceral adipose tissue physiology and increases inflammation

(A) Representative hematoxylin and eosin (H&E)-stained sections of visceral adipose tissue from adi-hRBP4 and littermate control (CTL) mice fed a high-fat diet. Bars represent 100 μm. Arrows indicate crown-like structures. (B) *Tnfα* mRNA expression in visceral adipose tissue was determined by qPCR (n = 6 - 11). Visceral fat (C) and plasma (D) TNFα protein levels and plasma leptin (E) levels were measured using commercial kits according to the manufacturers' instructions (n = 7 - 8). Data are expressed as means ± SEM. Bars not annotated with a common letter are statistically different ($P < 0.05$).

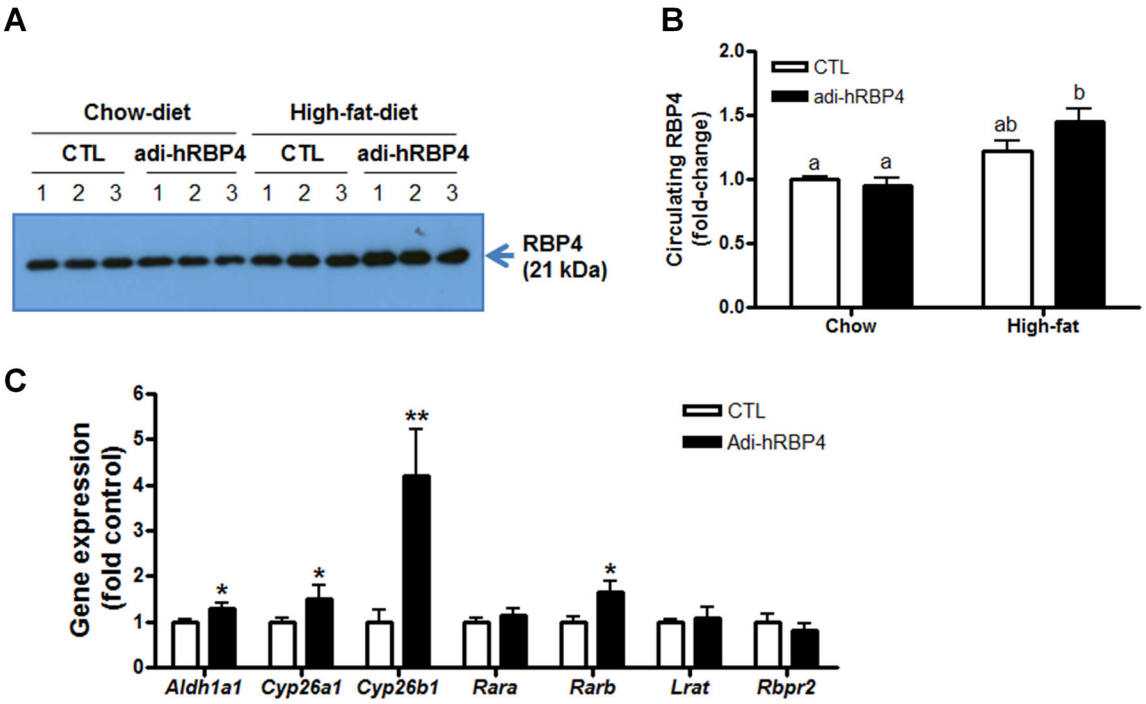

Figure 7. Plasma RBP4 levels were significantly increased in adi-hRBP4 mice fed a high-fat diet

(A) Immunoblots for RBP4 in plasma employing rabbit anti-rat RBP4 antibody that recognizes both mRBP4 and hRBP4. One-tenth of a microliter of plasma was loaded in each lane for RBP4 detection. (B) The relative protein expression level of RBP4 as determined from densiometric scans of the immunoblots. (C) Expression of genes involved in maintaining all-*trans*-retinoic acid levels were determined by qPCR (n = 4 - 6). *, $P < 0.05$ versus controls (CTL); **, $P < 0.01$ versus controls (CTL). Data are expressed as means ± SEM.

Table 1

Comparison of retinoid concentrations for male 4~5 month-old control and adi-hRBP4 mice fed a chow diet and a high-fat diet[1,2,3,4]

	Chow diet		High-fat diet	
Retinoid	**Control (n)**	**adi-hRBP4(n)**	**Control (n)**	**adi-hRBP4(n)**
		nmol/g, tissue		
Liver ROL	33.0 ± 13.7 (8)[a]	31.0 ± 11.8 (7)[a]	9.3 ± 0.8 (4)[b]	6.9 ± 1.2 (6)[b] **
RE	2388.9 ± 361.0 (8)[a]	2291.0 ± 105.1 (7)[a]	941.9 ± 228.5 (4)[b]	1155.0 ± 341.1 (6)[b]
VISC ROL	2.0 ± 0.4 (8)[a]	1.9 ± 0.4 (6)[a]	1.4 ± 0.4 (4)[a]	1.6 ± 0.3 (6)[a]
RE	6.1 ± 2.1 (8)[a]	6.0 ± 1.9 (6)[a]	1.3 ± 0.5 (4)[b]	1.6 ± 0.4 (6)[b]
		pmol/g, tissue		
Liver ATRA	17.7 ± 5.5 (6)[ab]	16.8 ± 6.2 (8)[a]	27.0 ± 6.9 (4)[b]	19.4 ± 2.1 (6)[ab] *
VISC ATRA	12.4 ± 5.3 (5)[a]	13.3 ± 4.0 (8)[a]	10.8 ± 2.1 (4)[a]	12.7 ± 3.9 (6)[a]
		μM		
Plasma ROL	1.2 ± 0.2 (8)[a]	1.4 ± 0.2 (7)[a]	2.5 ± 0.2 (4)[b]	2.9 ± 0.2 (5)[c] *

[1] After weaning, mice were maintained on a standard rodent diet chow until they reached 7-8 weeks of age and then fed either the same standard rodent diet chow or a diet providing 60% of calories as fat.

[2] The chow diet contains 15 IU of vitamin A, and the high-fat diet contains 4 IU of vitamin A.

[3] VISC, visceral adipose tissue; ROL, all-*trans*-retinol; RE, retinyl esters; ATRA, all-*trans*-retinoic acid.

[4] Data are given as means ± SD with n number in parenthesis; values within a row not sharing a common letter are statistically different (One-way ANOVA with Tukey post-test, $P < 0.05$);

* genotype effect on the same diet (Student's *t* test;

* $P < 0.05$;

** $P < 0.01$)